RSC Advances

PAPER

View Article Online
View Journal | View Issue

Cite this: *RSC Adv.*, 2017, **7**, 3152

Platelet-rich plasma ameliorates senescence-like phenotypes in a cellular photoaging model

Chuanlong Jia,†[a] Yongzhou Lu,†[a] Bo Bi,[b] Liang Chen,[a] Qingjian Yang,[a] Ping Yang,[a] Yu Guo,[a] Jingjing Zhu,[a] Ningwen Zhu[c] and Tianyi Liu*[a]

Background: Platelet-rich plasma (PRP) is a portion of blood plasma enriched with platelets widely investigated for accelerating bone and soft tissue healing. The purpose of this study is to evaluate the effects of PRP on the previous established photoaging model *in vitro* and to elucidate the potential anti-photoaging mechanisms of PRP. *Methods*: Murine dermal fibroblasts (MDFs) were isolated and cultured with or without PRP after exposure to repeated UVB irradiation per protocol. The senescent phenotypes were compared among groups, including cell morphology, senescence-associated β-galactosidase (SA-β-gal) expression, cell cycle arrest, production and degradation of extracellular matrix (ECM), ROS generation, and the alteration of major intracellular antioxidants. *Results*: 1% PRP effectively reduced the amount of flattened cells and significantly decreased the staining intensity as well as the percentage of SA-β-gal-positive cells when compared with UVB group. Furthermore, PRP appeared to prevent cell cycle arrest caused by irradiation by decreasing p53 and p21 expression. The PRP had demonstrated direct effects on ECM, including increase in type I collagen production and decrease in MMPs expression. Additionally, the increase of glutathione, one of the major intracellular antioxidants, induced by PRP provided a possible explanation for its therapeutic effect. *Conclusions*: Our work confirmed that PRP, a compound of various growth factors, could counteract senescence-like phenotypes at the cellular level, mirroring its rising clinical popularity in anti-aging and regenerative medicine. The promising effects of PRP calls for future study for further exploration of the underlying mechanisms, which will lead to a broadened application of PRP in future clinical use.

Received 14th November 2016
Accepted 12th December 2016

DOI: 10.1039/c6ra26725d

www.rsc.org/advances

1 Introduction

Extrinsic aging is induced by environmental factors, such as ultraviolet (UV) irradiation, smoke and common pollutants. Exposure to solar radiation, however, is the leading factor in extrinsic aging, also known as photoaging.[1,2] Dermal fibroblasts, as the predominant cell type in dermis, act to produce collagen and actively remodel the extracellular matrix (ECM). They play an important role in the process of photoaging and anti-aging especially when the skin is exposed to accumulated damage from UV irradiation.[3] The principal mechanisms of photoaging process include the accumulation of reactive oxygen species (ROS) and the increase of matrix metalloproteinases (MMPs) which are induced by ultraviolet irradiation on fibroblasts.[4,5] Considering the significant role of ROS and MMPs, one of the photoprotective strategies to prevent the damage of photoaging is to reduce the production of MMPs and to increase antioxidant components.

Platelet-rich plasma (PRP) has been used for stimulating wound healing and aiding tissue repair,[6,7] as they contain a host of powerful mitogenic and chemotactic growth factors. Platelets secrete at least seven essential growth factors involved in initiation of healing process, including platelet-derived growth factor (PDGF) isomers: PDGFaa, PDGFab and PDGFbb, transforming growth factor-β1 (TGF-β1), TGF-β2, vascular endothelial growth factor (VEGF), and epithelial growth factor (EGF). Along with the rapid evolvement of stem cell research, PRP has been widely investigated experimentally and clinically in recent years because of its various growth factors, which are considered the dominant effector of stem cell therapy. Several growth factors, including PDGF, bFGF and EGF, found in PRP have been showed to have positive effects on skin rejuvenation by stimulating the proliferation of fibroblasts *in vivo* and in animal studies.[8–10] Moreover, T. Kamakura *et al.* has proved that bFGF is effective in treating wrinkles and depressed areas of the skin of the face and body.[11] L. J. Xian *et al.* found that 10% PRP promoted wound remodeling and whereas the 20% PRP enhanced collagen deposition.[12] Q. Hui *et al.* further demonstrated that clinically PRP combined with ultra-pulsed

[a]*Department of Plastic and Reconstructive Surgery, Hua Dong Hospital, Fu Dan University, No. 221 West Yan'an Road, 200041 Shanghai, China. E-mail: tianyiliucn@126.com; Tel: +86 13162877696*

[b]*Department of Laboratory Medicine, Hua Dong Hospital, Fu Dan University, Shanghai, China*

[c]*Department of Dermatology, Hua Shan Hospital, Fu Dan University, Shanghai, China*

† These authors contributed equally to this work.

fractional CO_2 laser had a synergistic effect on facial rejuvenation.[13] However, the effects and potential mechanisms of PRP on photoaging fibroblasts, the key player in extrinsic aging, has been under investigated.

This study is aimed at testing the role of PRP on photoaging process at a cellular level and its potential mechanisms. We have previously developed a reproducible photo-damaged model of mouse dermal fibroblasts (MDFs) by repeated UVB exposures, which demonstrates a series of senescence-like phenotypes, including long-term growth arrest, flattened morphology, increased synthesis of MMPs, increased degradation of ECM and SA-β-gal staining.[14] With the utilization of the photoaging model, it is feasible to evaluate the definite effects of PRP on photoaging without confounding factors.

2 Materials and methods

Our study involves the use of live animals including rabbits and mice. Animals were adopted and promulgated in accordance with the guidelines of the China National Institutes of Health. And our experimental protocol was consented by Animal Care and Use Committee of Fudan University (Shanghai, China).

2.1 Preparation of PRP

A 25 ml whole blood was collected from the heart of a 3 month old healthy male New Zealand white rabbit under sterile conditions. 5 ml blood was counted using automatic blood analysis and the concentration of platelets was documented. 20 ml was processed to yield PRP using the two-step centrifugation at 4 °C, 215 g for 15 min followed by 863 g for 15 min. The supernatant above the packed cells contained two visibly different layers: the uppermost and nearly transparent layer containing platelet-poor plasma (PPP) and a lower partially flocculent layer containing PRP. From the final unit, approximately 2 ml of PRP could be collected. The PRP was used for the following study when platelet count of the PRP was 4 times more than that of the whole blood.

2.2 Cell culture and treatments

MDFs were isolated from the dorsal dermis of newborn littermates of C57 BL/6 mice 18–24 h after birth, as previously described.[15] The cells were maintained in DMEM supplemented with 10% fetal bovine serum (FBS), glutamine, penicillin and streptomycin in a 37 °C humidified incubator containing 5% CO_2. The fibroblasts were cultured to 80% confluence and then subcultured. Cells of passage 1–2 were used for the following experiments.

At 12 h after plating, the supernatant was replaced with a thin layer of phosphate-buffered saline (PBS) and cells were exposed to a series of 4 doses of UVB at 120 mJ cm^{-2} (Narrowband TL 20 W/01 RS lamp, Philips, The Netherlands) for 120 s with an interval time of 12 h as previously described.[16] Immediately after each irradiation, the PBS was aspirated and replaced with DMEM containing PRP in 1% FBS for treatment group. Control cells were kept in the same culture conditions without UVB exposure and/or PRP treatment. After a series of four exposures, the cells were allowed for recovery in DMEM with 10% FBS, and with PRP in treatment group.

2.3 Cell assays and the choice of PRP concentration

Normal cell proliferation of MDFs exposed to PRP (1% PRP, 5% PRP, 10% PRP which was diluted with 1% FBS) up to 48 h was determined using WST-8 dye (Cell Counting Kit-8, Beyotime Inst Biotech, China) according to the manufacturer's instructions. Briefly, 5×10^3 cells per well were seeded in a 96-well flat-bottomed plate. After 12 h, the medium was replaced with DMEM containing PRP of increasing doses and then cultured in a 37 °C humidified incubator containing 5% CO_2 for another 48 h. After incubation, 10 ml of WST-8 dye was added to each well, cells were incubated at 37 °C for 2 h and the absorbance was finally determined at 450 nm using Varioskan Flash Spectral Scanning Multimode Reader (Thermo Electron Corporation, USA). The alteration in viability of in PRP-treated fibroblasts was expressed as OD values compared to non-treated cells.

2.4 Morphology analysis by fluorescent labeling of cytoskeletal proteins

At 24 h after the last UVB treatment, cells were seeded in 35 mm dishes and cultivated for another 48 h in DMEM + 10% FBS. The cells were washed in PBS, fixed in 4% paraformaldehyde, permeabilized in 0.3% Triton X-100 for 15 min at room temperature, and then incubated with FITC-Phalloidin (Sigma Chemical Co, USA) for 30 min. Nuclei were identified with 40,6-diamidino-2-phenylindole (DAPI). Images were recorded at 400× using a fluorescent microscope (Olympus IX70-S1F2, Japan).

2.5 SA-β-gal staining

SA-β-gal staining was performed as previously described.[17] The staining kit was purchased from Cell Signaling Technology (#9860, Boston, MA, USA). At 24 h after the last UVB treatment, cells were seeded in 35 mm dishes and cultivated for another 48 h in DMEM + 10% FBS. The cells were washed in PBS, fixed for 10 min (room temperature) in 4% paraformaldehyde and stained according to the manufacturer's instruction. The population of SA-β-gal-positive cells was determined by counting 400 cells per dish using Image-Pro Plus (IPP) 6.0 software (Media Cybernetics, Bethesda, MD, USA). The proportions of cells positive for the SA-β-gal activity were given as percentage of the total number of cells counted in each dish.

2.6 Flow cytometry analysis for cell cycle

Cell-cycle analysis was performed by flow cytometry at 48 h after the last UVB treatment. Briefly, cultured cells were trypsinized into single-cell suspensions and fixed with 70% ethanol overnight at 4 °C. RNA was degraded by incubation with 1 mg ml^{-1} RNase (Sigma-Aldrich, St. Louis, MO, USA) for 1 h at 37 °C. DNA was labeled with 50 mg ml^{-1} propidium iodide (PI; Sigma-Aldrich) and DNA content was assessed by Beckman Coulter

Epics Altra flow cytometer (Beckman Coulter, High Wycombe, UK) equipped with the ModiFit LT v2.0 software.

2.7 RNA extraction and real-time RT-PCR

At 48 h after the last irradiation, total cellular RNA was extracted using TRIzol reagent (Invitrogen, Carlsbad, CA). cDNA was synthesized from 2 μg total RNA using 200 U of reverse transcriptase (MMLV RT) and 20 pM oligodT (Promega, Madison, WI). The primers were listed in Table 1. Amplification reactions assays contained 1× SYBR Green PCR Mastermix and primers (Applied Biosystems, The Netherlands) at optimal concentration. A hot start at 95 °C for 10 min was followed by 40 cycles at 95 °C for 30 s, 60 °C for 30 s and 72 °C for 45 s using the StrataGene Mx3000p (Agilent Technologies, USA). Melting curves were generated after amplification and data were analyzed using the Mxp software. Each sample was tested in triplicate and three independent repeating experiments were performed.

2.8 Protein quantification and western blotting

For quantification of soluble protein, cells were harvested at 72 h after the last UVB irradiation. The cell number was counted in each group and cells were lysed for quantification of protein using BCA kit (Pierce, USA). The amount of soluble protein was divided by cell numbers as a marker of cellular hypertrophy (protein/cell).

Western blot analysis was performed as previously described.[14] The total protein was extracted at 48 h after the PRP treatment. For cell-cycle regulatory proteins analysis, the cells were lysed at 72 h after the final stress. Total protein was prepared and subjected to 12% SDS-polyacryl-amide gel electrophoresis and subsequently transferred onto PVDF membranes. Blots were incubated with anti-p53, anti-p21, anti-collagen I antibody (all from Abcam, Cambridge, UK), washed and incubated with a secondary antibody conjugated to horseradish peroxidase. The bands were visualized chemiluminescently (Pierce, Rockford, USA).

2.9 Assessment of intracellular production of ROS

Intracellular ROS were determined with 20,70-dichlorodihydrofluoresce in diacetate ($DCFH_2$–DA; Sigma-Aldrich Co., LLC, USA). The cells were seeded in a 6-well flat bottom plate, pretreated with DMEM containing PRP for 48 h, washed with PBS and incubated with 5 mg ml^{-1} $DCFH_2$–DA for 20 min. The cells were then irradiated with UVB and subsequently analyzed by the fluorescence microscopy, Beckman Coulter Epics Altra flow cytometer (Beckman Coulter, High Wycombe, UK) equipped with the ModiFit LT v2.0 software, flow cytometer and Varioskan Flash Spectral Scanning Multimode Reader as previously described respectively. The fluorescence amount in PBS only group was used to be subtracted from the sample value of each corresponding well.

Table 1 Primers for RT-PCR

Collagen I	F	CCA GTG GCG GTT ATG ACT
	R	GCT GCG GAT GTT CTC AAT
MMP-1	F	ACT TTG AGA ACA CGG GGA
	R	CGG GGA TAA TCT TTG TCC
MMP-2	F	ATT CTG TCC CGA GAC CGC
	R	CAC CAC ACC TTG CCA TCG
MMP-3	F	CAA GGG ATG ATG ATG CTG GTA TGG
	R	TGG GAT TTC CTC CAT TTT GG
MMP-9	F	ACG ATA AGG ACG GCA AAT
	R	CA AAG ATG AAC GGG AAC AC
GAPDH	F	TGG TGA AGG TCG GTG TG
	R	GG TCA ATG AAG GGG TCG TT

2.10 Statistics

Statistical analyses were carried out using SPSS13.0 (Chicago, SPSS Inc.) software package. The paired Student's *t*-test was used for direct comparisons between UVB and UVB + PRP groups. For multiple comparisons, the one-way ANOVA was applied. All values were expressed as the mean ± SD, and $p < 0.05$ was considered significant.

3 Results

3.1 The response of normal and UVB-irradiated MDFs to PRP

To find out the optimal concentration of PRP for the subsequent experiments, we evaluated the proliferative effect of PRP on normal and UVB-treated MDFs at the same time, with PRP ranging from 1% to 10%. We found that PRP with different concentrations could promote cell proliferation when the cells were not exposed to UVB irradiation (Fig. 1A and B). In the UVB group, however, only 1% PRP was observed to increase the cell number and improve morphology as compared to 5% PRP and 10% PRP groups (Fig. 1C and D). Thus 1% PRP was used in the following experiments.

3.2 PRP reduced SA-β-gal staining

The cells were submitted to SA-β-gal staining 72 h after the last irradiation of UVB (Fig. 2A) to test whether PRP could prevent MDFs from acquiring characteristic senescent morphology. Our study revealed strong activity of SA-β-gal in UVB-treated MDFs, and reduced staining intensity in PRP treatment group. In addition, the proportion of positive cells was effectively decreased in PRP treatment group (Fig. 2B).

In accordance with the positive SA-β-gal staining result, we observed an enlarged and flattened senescent-like morphology in UVB irradiated cells (Fig. 2C) as visualized by phalloidin. The cells treated with 1% PRP showed smaller length and width as compared to UVB-treated cells. To quantify the extent of cell hypertrophy, we determined the soluble protein content per cell of each group. There was a 4-fold increase in protein per cell in UVB group as compared to control group, while the pretreatment of PRP led to a significant decline with regard to soluble protein level per cell (Fig. 2D).

3.3 PRP counteracted UVB-induced alteration of cell cycle in MDFs

To investigate the role of PRP on cell-cycle arrest induced by UVB, we firstly analyzed the DNA content labeled by propidium

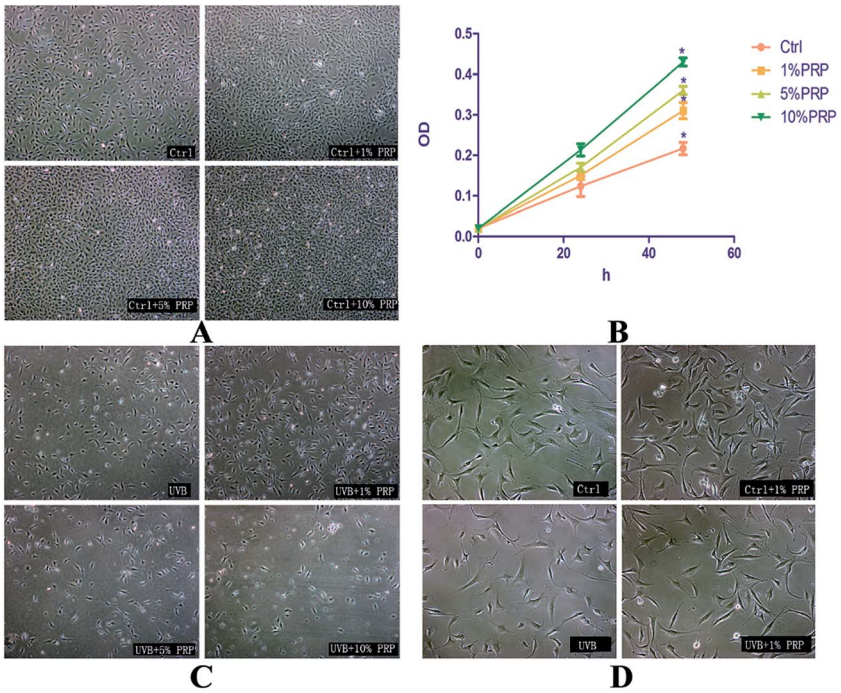

Fig. 1 Effects of PRP on the proliferation and morphology of normal and photoaging MDFs. Normal and photoaging MDFs were treated with PRP (1%, 5%, and 10%) for 48 h, and typical images were presented showing their cell density (A and C). The cell morphology of normal and photoaging cells with or without 1% PRP treatment was showed in (D). We used CCK-8 test, as showed in (B), to evaluate the proliferative activity of normal MDFs treated with various concentrations of PRP (1%, 5%, and 10%) for 48 h. Results were expressed as OD value ± SD.

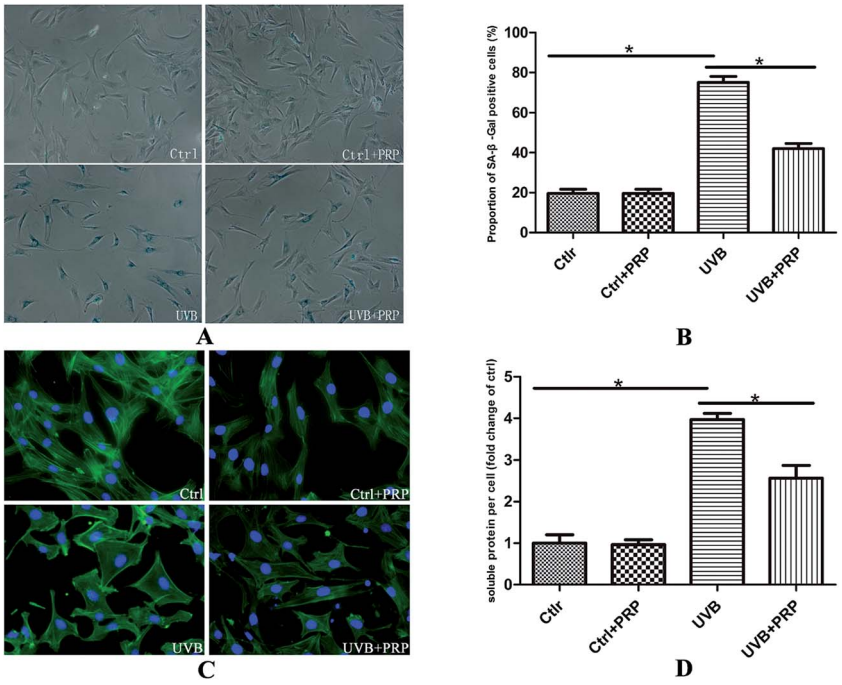

Fig. 2 Effects of PRP on SA-β-gal staining, cell morphology and hypertrophy. (A) At 72 h after the last exposure to UVB in the absence or presence of PRP, cells were fixed and stained for SA-β-gal. The SA-β-gal activity was found to be stained most intensively in perinuclear area. Original magnification × 100. (B) Proportion of cells positive for the SA-β-gal activity was determined by counting 400 cells per dish. Results are given as mean ± SD of three independent experiments (*$p < 0.05$). (C) At 72 h after the last irradiation, cells were fixed with 4% paraformaldehyde and their F-actin stained with FITC phalloidin. It was noteworthy that UVB group had more diverse morphotypes, and 1% PRP was found to ameliorate the typical senescent morphology, presenting as less flattened cells with some preserved spindled shape. Original magnification × 200. (D) After 72 h, the cells were trypsinized and counted. In parallel, cells were lysed for immunoblot and soluble protein content was measured for each group. The amount of soluble protein was divided by cell numbers as a marker of cellular hypertrophy (protein/cell). The result was shown as folds compared with control group. Results represent the mean ± SD of triplicate determinations (*$p < 0.05$).

iodide in each group at 48 h after the last irradiation. In consistence with our previous report, UVB group showed a decreased cell population in G0/G1 and G2/M phases (from 81.6 ± 1.21 to 73.3 ± 2.18% and 10.4 ± 0.75 to 6.72 ± 1.26%) and an increased cell population in S phase (from 7.92 ± 1.21 to 20 ± 2.3%) as compared to control cells. We further found that PRP was capable of preventing the cell cycle alteration to some extent in S phase as compared to UVB group (from 20 ± 2.3% to 11.2 ± 0.92%) (Fig. 3A).

Next, we sought to determine the level of p53 and p21, which were critical cell-cycle regulators and up-regulated in senescent cells,[18,19] at 48 h after the last irradiation. The expression of p53 and p21 was significantly enhanced in UVB treated MDFs, as assessed by western blotting analysis (Fig. 3B and C). Notably, p21 and p53 in UVB group showed a significant increase as compared with the control group. PRP was showed to have counteracted the induction of p21 and p53 expression in PRP treatment group compared to those exposed to UVB only.

In photoaging, decreased type I collagen expression and increased MMPs, such as MMP-1, -2, -3, and -9, are characteristic change. It led us to test the possible effects of PRP on collagen and MMPs expression. At 48 h after the last irradiation, we observed a significant increase in the expression of MMPs, including MMP-1, -2, -3, and -9 (Fig. 4A) at the mRNA level and a relevant decrease in type I collagen expression at the mRNA (Fig. 4B) and protein (Fig. 4C) levels at UVB group. Administration with PRP significantly decreased the release of MMP-1, -3, and -9, but not MMP-2, at the mRNA level (Fig. 4A). It also partly counteracted the UVB induced down-modulation of type I collagen at the mRNA and protein levels (Fig. 4B and C) at UVB plus PRP group.

3.4 PRP treatment down-modulated UVB-induced ROS accumulation and promoted the expression of antioxidant genes in MDFs

To clarify the potential mechanism of PRP in the rescue of photo-damaged MDFs, we first assessed the intracellular level of ROS generated by UVB in MDFs. In accordance with our previous report,[14] a single exposure to subcytotoxic dose of UVB resulted in a progressive accumulation of intracellular ROS which peaked at 30 minutes after the UVB irradiation (Fig. 5A). The presence of PRP significantly reduced the fluorescence intensity at 30 minutes, as evident by the curve of PRP group shifting to the left detected by Beckman Coulter Epics Altra flow cytometer (Fig. 5B) and the value of fluorescence intensity lowered apparently detected by Varioskan Flash Spectral Scanning Multimode Reader (Fig. 5C). Furthermore, we sought to determine the major intracellular antioxidants by measuring the protein levels in UVB group with or without PRP treatment. Here we demonstrated that PRP induced a 2.7-fold increase of glutathione (GPx), but not catalase (CAT), superoxide dismutase 1 (SOD1) or superoxide dismutase 2 (SOD2) after 48 h treatment (Fig. 5D).

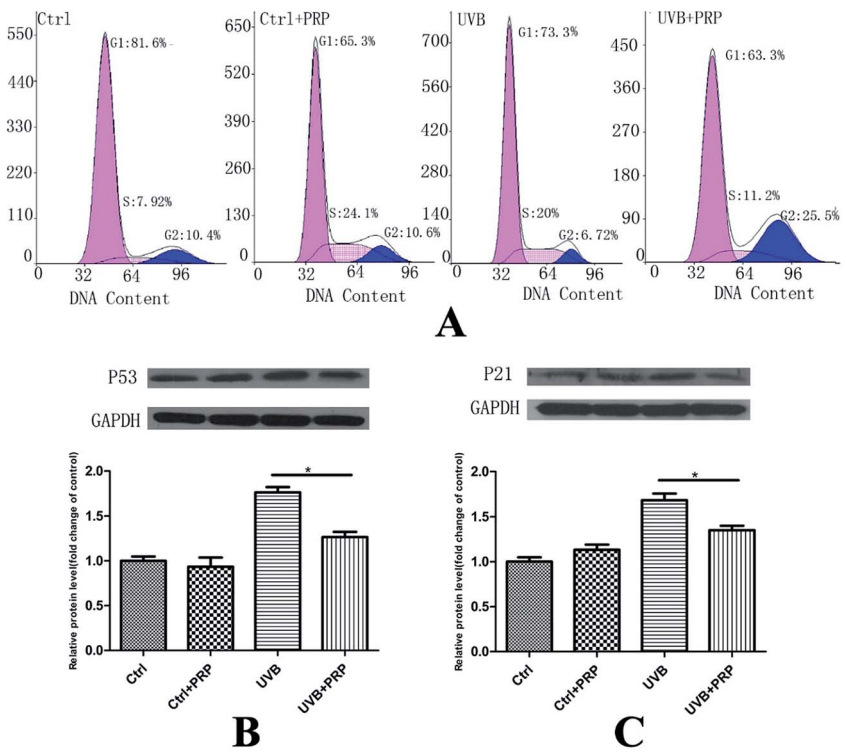

Fig. 3 Effect of PRP on UVB-induced alteration of cell cycle in MDFs. (A) At 48 h after the last irradiation, the cells were collected and the cell cycle was analyzed by flow cytometry using propidium iodide staining. (B and C) Western blotting analysis of each group for p53 (B) and p21 (C) at 72 h after the last UVB irradiation. The protein level was quantified using GAPDH as a reference and expressed as 100% of the protein level in control cells. Each bar represents mean ± SD from three samples (*$p < 0.05$) and a representative image from three independent experiments of western blotting analysis was shown.

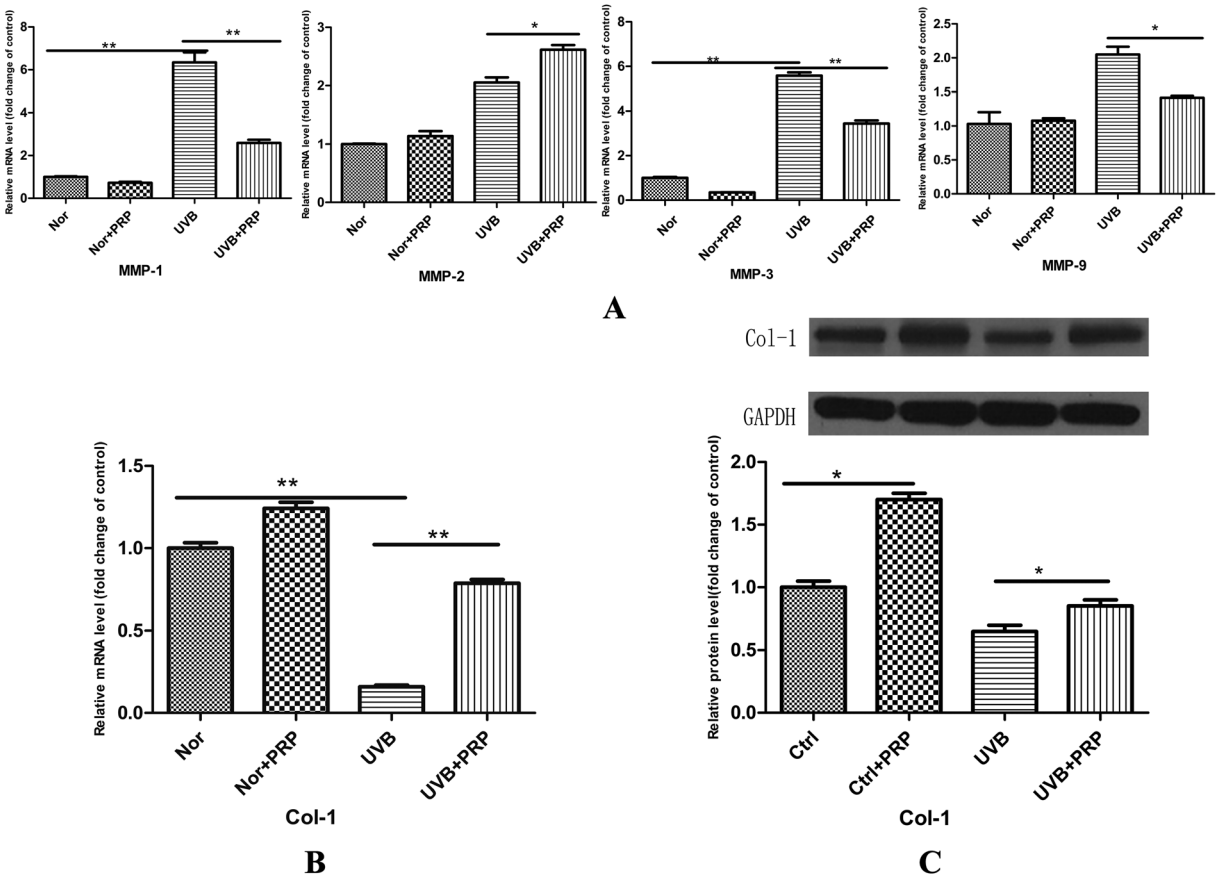

Fig. 4 Effect of PRP on UVB-induced dermal matrix alterations in MDFs. (A and B) Real-time RT-PCR analysis of each group for MMPs, including MMP-1, -2, -3 and -9 (A) and collagen I (B) at 48 h after the last UVB irradiation. The mRNA level was quantified using GAPDH as a reference and expressed as 100% of the mRNA level in control cells, and the results represent the mean ± SD of triplicate determinations (*$p < 0.05$). (C) Western blotting analysis of each group for collagen I at 72 h after the last UVB irradiation. The protein level was quantified using GAPDH as a reference and expressed as 100% of the protein level in control cells. Each bar represents mean ± SD from three samples (*$p < 0.05$) and a representative image from three independent experiments of western blotting analysis was shown.

4 Discussion

Photoaging is a cutaneous degenerative process superimposed on intrinsic aging and results predominantly from the effect of solar ultraviolet (UV) that can induce overexpression of ROS and MMPs in dermal fibroblasts, which play an important role in the remodeling of ECM.[5] The strategies to prevent or reduce the deleterious effect of UV have largely targeted at preventing UV from penetrating the skin to reduce its detrimental effects on skin appearance.[20] Alternatively, reduction of oxidative stress or enhancement of antioxidant system in fibroblasts has been proposed to be a potential anti-aging technique.[21–23] Many studies have established a variety of exogenous compounds with the ability to promote endogenous protective responses in order to decrease the damage of oxidative stress.[24,25] Based on previous reports of PRP with its promising effects on regenerative medicine due to its various growth factors, we investigated the possibility of using PRP to promote skin rejuvenation by influencing the dermal fibroblasts.[26–28] Previously, J. M. Cho *et al.* found that PRP was effective in the rejuvenation of photoaged skin in a nude mice model.[29] M. K. Shin *et al.* demonstrated that PRP increased the amount of collagen and the number of normal fibroblasts.[30] P. Mehryan *et al.* has proved that PRP had the ability to ameliorate dark pigmentation on skin.[31] In accordance with the above-mentioned studies, we demonstrated that the biological factors contained in PRP played an important role in the process of anti-aging. In a word, these factors could stimulate the proliferation and migration of fibroblasts, up-regulate the collagen production and decrease MMPs expression, and show protective effects from UVB damages by enhancing intracellular antioxidants.

In our study, we found that PRP was able to counteract some characteristics of UVB-induced senescence in MDFs. UVB-irradiated MDFs treated with PRP has preserved elongated cell shape and revealed significant decrease in the staining intensity and in the percentage of SA-β-gal-positive cells. Additionally, the anti-senescent effects of PRP were supported by counteraction of cell-cycle arrest and repression of the expression of UVB-induced p53 and p21. Our previous study[16] has shown that UVB induces S-phase arrest, which seems be resulted from blunt interruption of DNA replication in rapidly proliferating cells. The induction of expression of p53 and p21 helps avoid the replication of damaged DNA and thus minimizes the possibility of introducing gene mutations in daughter cells.[32–35]

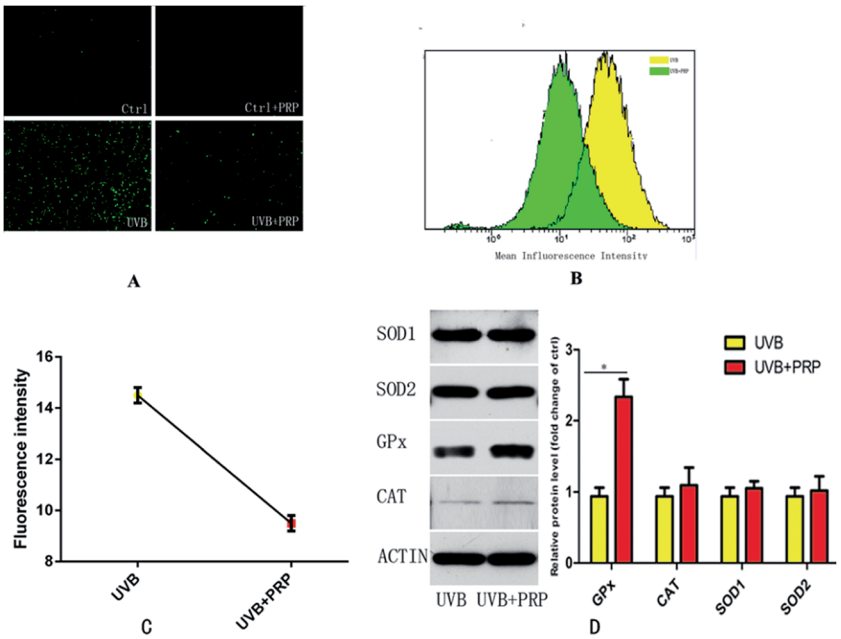

Fig. 5 Effects of PRP on the UVB-induced ROS accumulation and antioxidant defense in MDFs. (A) The cells were treated in the absence or presence of PRP for 48 h, and then exposed to UVB irradiation or PBS treatment only after 20 min incubation with 5 mg ml^{-1} $DCFH_2$–DA. Original magnification × 40. (B) Flow cytometry analysis for mean fluorescence intensity between UVB and UVB + PRP group after 30 min incubation with 5 mg ml^{-1} $DCFH_2$–DA. The mean fluorescence intensity of two groups was showed in different colors. (C) Fluorescence microplate for mean fluorescence intensity between UVB and UVB + PRP group after 30 min incubation with 5 mg ml^{-1} $DCFH_2$–DA. (D) Western Blotting analysis for CAT, SOD1, SOD2 and GPx after 48 h treatment in the absence or presence of PRP. The protein level was quantified using actin as a reference and expressed as fold change of the protein level in control cells. The results represent the mean ± SD of triplicate determinations (*p < 0.05).

Aging skin usually presents with changes in pigmentation, sallowness, and deep wrinkling. The underlying alteration includes increased collagen breakdown and degradation from MMPs. Many studies have shown that the synthesis of MMPs of human or mouse skin, such as MMP-1, -2, -3, and -9, are upregulated when exposed to UV irradiation.[36–38] In our study, the expression of MMP-1 (collagenase), MMP-2 (gelatinase A), MMP-3 (stromelysin) and MMP-9 (gelatinase B), and collagen-1 which constitute 85–90% of the total ECM,[39] were detected. We here demonstrated that PRP inhibited the degradation of collagen-1 from UVB irradiation by decreasing MMP-1, -3, -9. Interestingly, PRP treatment appeared to cause increased MMP-2, which has gained the attention in our ongoing study. Our preliminary data showed that MMP-2 might play a different role in photoaging.

Furthermore, we investigated the possible molecular mechanisms of the anti-photoaging effects of PRP. ROS induced by UV facilitate peroxidation of the lipid components of the cell membrane, which cause the alterations of several antioxidant enzymatic systems.[40] Excessive oxidative stress and imbalanced anti-oxidative system play an important role in the process of cellular senescence.[41] Given the fact that oxidative stress has been demonstrated as one of the most important culprits in cellular senescence, we proposed that PRP might preserve the MDFs function by decreasing the accumulation of ROS at the cellular level. Our results confirmed that PRP reduced UVB-induced accumulation of ROS by enhancing the activity of intracellular antioxidant enzymes, mainly GPx. The mechanism of action of PRP is implied as the effect of its plentiful content of platelets and growth factors which can trigger cell activation and activate related signal path. Growth factors including PDGF, VEGF and the adhesive glycoproteins secreted from the activated platelets interact with the cells by binding to their specific cellular membrane receptors. After that, the glycoproteins and the growth factors activate intracellular processes that stimulate cell proliferation, migration, survival and the production of extracellular matrix proteins particularly new collagen formation.[42] The downstream complex interactions between growth factors present in PRP that has been reported as anti-oxidative factors, such as IGF, which was confirmed to have the ability to repair impaired RNA and DNA and reduce the degree of oxidative stress.[43,44] PDGF, IGF, and HGF, seems to increase the level of resistance to oxidation by activating the PI3K/Akt pathway which can reduce ROS production.[45–50]

In conclusion, our study demonstrated that PRP, as a compound of multiple factors, ameliorated senescence-like phenotypes, including flattened morphology, long-term growth arrest, SA-β-gal staining. PRP also prevented the degradation of ECM by inhibiting the expression of MMPs and increasing the collagen production. The activity of GPx as one of the most important antioxidants was increased by PRP treatment. To our knowledge, this is the first study focusing on the anti-aging effects of PRP at a cellular level, which provide us an insight on its possible future application in skin rejuvenation.

However, further studies are prompted to illustrate the key factors and their signaling pathways underlying the observed anti-aging effects.

Acknowledgements

This work was supported by grants from National Natural Science Foundation of China (81272125, 81301642), Program of Shanghai Medicine Subject Chief Scientist (2011033) and National High Technology Research and Development Program of China (SS2014AA020705). We would like to acknowledge the help of all the staff at Shanghai Key Laboratory of Tissue Engineering.

References

1 D. Bernhard, C. Moser, A. Backovic and G. Wick, Cigarette smoke–an aging accelerator?, *Exp. Gerontol.*, 2007, **42**, 160–165.
2 M. Wlaschek, I. Tantcheva-Poor, L. Naderi, W. Ma, L. A. Schneider, Z. Razi-Wolf, J. Schuller and K. Scharffetter-Kochanek, Solar UV irradiation and dermal photoaging, *J. Photochem. Photobiol., B*, 2001, **63**, 41–51.
3 G. J. Fisher, J. Varani and J. J. Voorhees, Looking older: fibroblast collapse and therapeutic implications, *Arch. Dermatol.*, 2008, **144**, 666–672.
4 B. A. Gilchrest, Photoaging, *J. Invest. Dermatol.*, 2013, **133**, E2–E6.
5 E. Kohl, J. Steinbauer, M. Landthaler and R. M. Szeimies, Skin ageing, *J. Eur. Acad. Dermatol. Venereol.*, 2011, **25**, 873–884.
6 M. Qiu, D. Chen, C. Shen, J. Shen, H. Zhao and Y. He, Platelet-Rich Plasma-Loaded Poly(D,L-lactide)-Poly(ethylene glycol)-Poly(D,L-lactide) Hydrogel Dressing Promotes Full-Thickness Skin Wound Healing in a Rodent Model, *Int. J. Mol. Sci.*, 2016, **17**, 1001.
7 P. Gentile, B. De Angelis, A. Agovino, F. Orlandi, A. Migner, C. Di Pasquali and V. Cervelli, Use of Platelet Rich Plasma and Hyaluronic Acid in the Treatment of Complications of Achilles Tendon Reconstruction, *World J. Plast. Surg.*, 2016, **5**, 124–132.
8 Z. D. Draelos, The Effect of a Combination of Recombinant EGF Cosmetic Serum and a Crosslinked Hyaluronic Acid Serum as Compared to a Fibroblast-Conditioned Media Serum on the Appearance of Aging Skin, *J. Drugs Dermatol.*, 2016, **15**, 738–741.
9 S. Fabi and H. Sundaram, The potential of topical and injectable growth factors and cytokines for skin rejuvenation, *Facial Plast. Surg.*, 2014, **30**, 157–171.
10 F. Passaretti, M. Tia, V. D'Esposito, M. De Pascale, C. M. Del, R. Sepulveres, D. Liguoro, R. Valentino, F. Beguinot, P. Formisano and G. Sammartino, Growth-promoting action and growth factor release by different platelet derivatives, *Platelets*, 2014, **25**, 252–256.
11 T. Kamakura, J. Kataoka, K. Maeda, H. Teramachi, H. Mihara, K. Miyata, K. Ooi, N. Sasaki, M. Kobayashi and K. Ito, Platelet-Rich Plasma with Basic Fibroblast Growth Factor for Treatment of Wrinkles and Depressed Areas of the Skin, *Plast. Reconstr. Surg.*, 2015, **136**, 931–939.
12 L. J. Xian, S. Roy Chowdhury, A. Bin Saim and R. Bt Hj Idrus, Concentration-dependent effect of platelet-rich plasma on keratinocyte and fibroblast wound healing, *Cytotherapy*, 2015, **17**, 293–300.
13 Q. Hui, P. Chang, B. Guo, Y. Zhang and K. Tao, The Clinical Efficacy of Autologous Platelet-Rich Plasma Combined with Ultra-Pulsed Fractional CO_2 Laser Therapy for Facial Rejuvenation, *Rejuvenation Res.*, 2016, 1823.
14 J. P. Zeng, B. Bi, L. Chen, P. Yang, Y. Guo, Y. Q. Zhou and T. Y. Liu, Repeated exposure of mouse dermal fibroblasts at a sub-cytotoxic dose of UVB leads to premature senescence: a robust model of cellular photoaging, *J. Dermatol. Sci.*, 2014, **73**, 49–56.
15 H. Fujisawa, T. Nishikawa, B. H. Zhu, N. Takeda, H. Jujo, K. Higuchi and M. Hosokawa, Accelerated aging of dermal fibroblast-like cells from the senescence-accelerated mouse (SAM): acceleration of changes in DNA ploidy associated with *in vitro* cellular aging, *J. Gerontol., Ser. A*, 1998, **53**, B11–B17.
16 J. Zeng, B. Bi, L. Chen, P. Yang, Y. Guo, Y. Zhou and T. Liu, Repeated exposure of mouse dermal fibroblasts at a sub-cytotoxic dose of UVB leads to premature senescence: a robust model of cellular photoaging, *J. Dermatol. Sci.*, 2014, **73**, 49–56.
17 G. P. Dimri, X. Lee, G. Basile, M. Acosta, G. Scott, C. Roskelley, E. E. Medrano, M. Linskens, I. Rubelj, O. Pereira-Smith, *et al.*, A biomarker that identifies senescent human cells in culture and in aging skin *in vivo*, *Proc. Natl. Acad. Sci. U. S. A.*, 1995, **92**, 9363–9367.
18 Z. Zhang, H. He, F. Chen, C. Huang and X. Shi, MAPKs mediate S phase arrest induced by vanadate through a p53-dependent pathway in mouse epidermal C141 cells, *Chem. Res. Toxicol.*, 2002, **15**, 950–956.
19 G. Wu, N. Lin, L. Xu, B. Liu and M. A. Feitelson, UCN-01 induces S and G2/M cell cycle arrest through the p53/p21(waf1) or CHK2/CDC25C pathways and can suppress invasion in human hepatoma cell lines, *BMC Cancer*, 2013, **13**, 167.
20 M. F. Holick, Sunlight, UV-radiation, vitamin D and skin cancer: how much sunlight do we need?, *Adv. Exp. Med. Biol.*, 2008, **624**, 1–15.
21 S. Q. Wang, Photoprotection: a Review of the Current and Future Technologies, *Dermatol. Ther.*, 2010, **23**, 31–47.
22 Z. A. Abdel-Malek, A. L. Kadekaro and V. B. Swope, Stepping up melanocytes to the challenge of UV exposure, *Pigm. Cell Melanoma Res.*, 2010, **23**, 171–186.
23 S. González, M. Fernández-Lorente and Y. Gilaberte-Calzada, The latest on skin photoprotection, *Clin. Dermatol.*, 2008, **26**, 614–626.
24 A. Svobodova and J. Vostalova, Solar radiation induced skin damage: review of protective and preventive options, *Int. J. Radiat. Biol.*, 2010, **86**, 999–1030.
25 X. Song, N. Mosby, J. Yang, A. Xu, Z. Abdel-Malek and A. L. Kadekaro, Alpha-MSH activates immediate defense

responses to UV-induced oxidative stress in human melanocytes, *Pigm. Cell Melanoma Res.*, 2009, **22**, 809–818.
26 C. E. Martínez, P. C. Smith and V. A. Palma Alvarado, The influence of platelet-derived products on angiogenesis and tissue repair: a concise update, *Front Physiol*, 2015, **6**, 290.
27 I. Andia and N. Maffulli, Platelet-rich plasma for managing pain and inflammation in osteoarthritis, *Nat. Rev. Rheumatol.*, 2013, **9**, 721–730.
28 E. Galliera, M. M. Corsi and G. Banfi, Platelet rich plasma therapy: inflammatory molecules involved in tissue healing, *J. Biol. Regul. Homeostatic Agents*, 2012, **26**, 35S–42S.
29 J. M. Cho, Y. H. Lee, R. M. Baek and S. W. Lee, Effect of platelet-rich plasma on ultraviolet b-induced skin wrinkles in nude mice, *J. Plast. Reconstr. Aesthetic Surg.*, 2011, **64**, e31–e39.
30 M. K. Shin, J. H. Lee, S. J. Lee and N. I. Kim, Platelet-rich plasma combined with fractional laser therapy for skin rejuvenation, *Dermatol. Surg.*, 2012, **38**, 623–630.
31 P. Mehryan, H. Zartab, A. Rajabi, N. Pazhoohi and A. Firooz, Assessment of efficacy of platelet-rich plasma (PRP) on infraorbital dark circles and crow's feet wrinkles, *J. Cosmet., Dermatol. Sci. Appl.*, 2014, **13**, 72–78.
32 K. Itahana, G. P. Dimri, E. Hara, Y. Itahana, Y. Zou, P. Y. Desprez and J. Campisi, A Role for p53 in Maintaining and Establishing the Quiescence Growth Arrest in Human Cells, *J. Biol. Chem.*, 2002, **277**, 18206–18214.
33 S. J. Kuerbitz, B. S. Plunkett, W. V. Walsh and M. B. Kastan, Wild-type p53 is a cell cycle checkpoint determinant following irradiation, *Proc. Natl. Acad. Sci. U. S. A.*, 1992, **89**, 7491–7495.
34 Y. Cho, S. Gorina, P. D. Jeffrey and N. P. Pavletich, Crystal structure of a p53 tumor suppressor-DNA complex: understanding tumorigenic mutations, *Science*, 1994, **265**, 346–355.
35 J. Brugarolas, C. Chandrasekaran, J. I. Gordon, D. Beach, T. Jacks and G. J. Hannon, Radiation-induced cell cycle arrest compromised by p21 deficiency, *Nature*, 1995, **377**, 552–557.
36 F. Debacq-Chainiaux, C. Leduc, A. Verbeke and O. Toussaint, UV, stress and aging, *Derm.-Endocrinol.*, 2012, **4**, 236–240.
37 S. Inomata, Y. Matsunaga, S. Amano, K. Takada, K. Kobayashi, M. Tsunenaga, T. Nishiyama, Y. Kohno and M. Fukuda, Possible involvement of gelatinases in basement membrane damage and wrinkle formation in chronically ultraviolet B-exposed hairless mouse, *J. Invest. Dermatol.*, 2003, **120**, 128–134.
38 P. K. Vayalil, A. Mittal, Y. Hara, C. A. Elmets and S. K. Katiyar, Green Tea Polyphenols Prevent Ultraviolet Light-Induced Oxidative Damage and Matrix Metalloproteinases Expression in Mouse Skin, *J. Invest. Dermatol.*, 2004, **122**, 1480–1487.
39 J. H. Chung, S. H. Youn, O. S. Kwon, K. H. Cho, J. I. Youn and H. C. Eun, Regulations of collagen synthesis by ascorbic acid, transforming growth factor-beta and interferon-gamma in human dermal fibroblasts cultured in three-dimensional collagen gel are photoaging- and aging-independent, *J. Dermatol. Sci.*, 1997, **15**, 188–200.
40 M. Yaar and B. A. Gilchrest, Photoaging: mechanism, prevention and therapy, *Br. J. Dermatol.*, 2007, **157**, 874–887.
41 S. Briganti, E. Flori, A. Mastrofrancesco, D. Kovacs, E. Camera, M. Ludovici, G. Cardinali and M. Picardo, Azelaic acid reduced senescence-like phenotype in photo-irradiated human dermal fibroblasts: possible implication of PPARgamma, *Exp. Dermatol.*, 2013, **22**, 41–47.
42 D. H. Kim, Y. J. Je, C. D. Kim, Y. H. Lee, Y. J. Seo, J. H. Lee and Y. Lee, Can Platelet-rich Plasma Be Used for Skin Rejuvenation? Evaluation of Effects of Platelet-rich Plasma on Human Dermal Fibroblast, *Ann. Dermatol.*, 2011, **23**, 424–431.
43 G. Schmidmaier, B. Wildemann, J. Heeger, T. Gabelein, A. Flyvbjerg, H. J. Bail and M. Raschke, Improvement of fracture healing by systemic administration of growth hormone and local application of insulin-like growth factor-1 and transforming growth factor-beta1, *Bone*, 2002, **31**, 165–172.
44 T. Molloy, Y. Wang and G. Murrell, The roles of growth factors in tendon and ligament healing, *Sports Med.*, 2003, **33**, 381–394.
45 L. Zheng, Y. Ishii, A. Tokunaga, T. Hamashima, J. Shen, Q. L. Zhao, S. Ishizawa, T. Fujimori, Y. Nabeshima, H. Mori, T. Kondo and M. Sasahara, Neuroprotective effects of PDGF against oxidative stress and the signaling pathway involved, *J. Neurosci. Res.*, 2010, **88**, 1273–1284.
46 J. Kajstura, F. Fiordaliso, A. M. Andreoli, B. Li, S. Chimenti, M. S. Medow, F. Limana, B. Nadal-Ginard, A. Leri and P. Anversa, IGF-1 overexpression inhibits the development of diabetic cardiomyopathy and angiotensin II-mediated oxidative stress, *Diabetes*, 2001, **50**, 1414–1424.
47 N. Baregamian, J. Song, M. G. Jeschke, B. M. Evers and D. H. Chung, IGF-1 protects intestinal epithelial cells from oxidative stress-induced apoptosis, *J. Surg. Res.*, 2006, **136**, 31–37.
48 M. I. Niagara, H. Haider, S. Jiang and M. Ashraf, Pharmacologically preconditioned skeletal myoblasts are resistant to oxidative stress and promote angiomyogenesis *via* release of paracrine factors in the infarcted heart, *Circ. Res.*, 2007, **100**, 545–555.
49 Y. J. Zhou, H. W. Yang, X. G. Wang and H. Zhang, Hepatocyte growth factor prevents advanced glycation end products-induced injury and oxidative stress through a PI3K/Akt-dependent pathway in human endothelial cells, *Life Sci.*, 2009, **85**, 670–677.
50 L. Hui, Y. Hong, Z. Jingjing, H. Yuan, C. Qi and Z. Nong, HGF suppresses high glucose-mediated oxidative stress in mesangial cells by activation of PKG and inhibition of PKA, *Free Radical Biol. Med.*, 2010, **49**, 467–473.

